biology

MDPI

Article

Network Pharmacology Reveals *Curcuma aeruginosa* Roxb. Regulates MAPK and HIF-1 Pathways to Treat Androgenetic Alopecia

Aaron Marbyn L. Sintos [1] and Heherson S. Cabrera [1,2,*]

[1] School of Chemical, Biological, and Materials Engineering and Sciences, Mapúa University, Manila 1002, Philippines; amlsintos@mymail.mapua.edu.ph
[2] Department of Biology, School of Health Sciences, Mapúa University, Makati 1200, Philippines
* Correspondence: hscabrera@mapua.edu.ph

Simple Summary: Androgenetic alopecia (AGA) represents the most common form of hair loss experienced by both men and women. *Curcuma aeruginosa* Roxb., a plant known for its medicinal properties, has shown promise in reversing this hair loss disorder for its hair growth effects and anti-androgenic effects. Despite its promising potential, the mechanism of action by which it acts remains unknown. As such, this study unveiled how this plant works against hair loss by identifying its bioactive compounds, the gene its targets, and the potential mechanism involved in the therapy of AGA using network pharmacology and molecular docking. The findings revealed insights into how *C. aeruginosa* can potentially prevent AGA, highlighting its potential for developing new, safe therapies for AGA, benefiting those affected by this condition.

Abstract: Androgenetic alopecia (AGA) is the most prevalent hair loss disorder worldwide, driven by excessive sensitivity or response to androgen. Herbal extracts, such as *Curcuma aeruginosa* Roxb., have shown promise in AGA treatment due to their anti-androgenic activities and hair growth effects. However, the precise mechanism of action remains unclear. Hence, this study aims to elucidate the active compounds, putative targets, and underlying mechanisms of *C. aeruginosa* for the therapy of AGA using network pharmacology and molecular docking. This study identified 66 bioactive compounds from *C. aeruginosa*, targeting 59 proteins associated with AGA. Eight hub genes were identified from the protein–protein interaction network, namely, CASP3, AKT1, AR, IL6, PPARG, STAT3, HIF1A, and MAPK3. Topological analysis of components–targets network revealed trans-verbenol, myrtenal, carvone, alpha-atlantone, and isoaromandendrene epoxide as the core components with potential significance in AGA treatment. The molecular docking verified the binding affinity between the hub genes and core compounds. Moreover, the enrichment analyses showed that *C. aeruginosa* is involved in hormone response and participates in HIF-1 and MAPK pathways to treat AGA. Overall, this study contributes to understanding the potential anti-AGA mechanism of *C. aeruginosa* by highlighting its multi-component interactions with several targets involved in AGA pathogenesis.

Keywords: androgenetic alopecia; *Curcuma aeruginosa* Roxb.; network pharmacology; molecular docking; protein–protein interaction network; enrichment analyses

check for updates

Citation: Sintos, A.M.L.; Cabrera, H.S. Network Pharmacology Reveals *Curcuma aeruginosa* Roxb. Regulates MAPK and HIF-1 Pathways to Treat Androgenetic Alopecia. *Biology* **2024**, *13*, 497. https://doi.org/10.3390/biology13070497

Academic Editor: Armando Varela-Ramirez

Received: 1 June 2024
Revised: 20 June 2024
Accepted: 26 June 2024
Published: 4 July 2024

Copyright: © 2024 by the authors. Licensee MDPI, Basel, Switzerland. This article is an open access article distributed under the terms and conditions of the Creative Commons Attribution (CC BY) license (https://creativecommons.org/licenses/by/4.0/).

1. Introduction

Androgenic alopecia (AGA) is the most prevalent hair loss disorder, causing at least 95% of all pattern hair loss cases, such as hair thinning among women and baldness in men [1]. AGA, an androgen-dependent alopecia with genetic origin, features progressive replacement of thick, long terminal hair with fine, small vellus hair. The androgens responsible for AGA are testosterone and its biologically active metabolite, dihydrotestosterone

(DHT). High levels of, or hypersensitivity to, DHT miniaturizes hair follicles, causing a shortened anagen phase of the hair growth cycle and, eventually, hair loss.

Although AGA does not pose a significant health risk, it may affect an individual's mental and social well-being, amplifying the need for treatment [2]. Currently, only two drugs are approved by the Food and Drug Administration (FDA) to treat AGA, namely, oral finasteride and topical minoxidil. Although they exhibited favorable efficacy, side effects are reported, such as sexual dysfunction from finasteride [3] and dermatitis from minoxidil [4]. Because of this, many opt for complementary and alternative medicine (CAM) interventions. One of these is the use of herbal extracts, which have been shown to stop hair loss and encourage hair growth [5].

Curcuma aeruginosa Roxb. is a rhizomatous plant rich in ethnomedicinal values for treating several ailments, exhibiting a wide spectrum of pharmacologic activities such as antioxidant [6], anti-cancer [7], antimicrobial [8], anti-HIV-1 [9], uterine-relaxant [10], and anti-androgenic effects. Phytochemically, *C. aeruginosa* is a rich source of sesquiterpenes, which have been shown to exhibit anti-androgenic action in vitro and in vivo by suppressing the growth of testosterone-induced human prostate cancer cells and androgen-dependent hamster flank gland model, respectively [11]. Additionally, clinical trials have demonstrated that *C. aeruginosa* is a promising, efficient component of AGA hair tonic for slowing hair loss and stimulating hair growth [12,13]. Despite exhibiting therapeutic effects on AGA, the mechanism by which *C. aeruginosa* acts remains unknown.

Therefore, the purpose of this study is to elucidate the potential mechanism of *C. aeruginosa* against AGA through network pharmacology and molecular docking. Network pharmacology has become a commonly used tool in drug research to unveil how drugs interact with their targets, pathways, and associated disorders [14]. Meanwhile, molecular docking is utilized to confirm the potential associations of compounds and target genes predicted in the network pharmacological analysis [15].

This study is limited to investigating the influence of *C. aeruginosa* on AGA using an in silico approach, as none had been reported. Initially, the bioactive compounds of the said plant were screened out and selected. The overlap between its predicted targets and AGA-linked target genes was acquired for protein–protein interaction (PPI) construction and GO and KEGG enrichment analyses. Furthermore, the components–targets–pathways network was visualized to give a general overview of the molecular mechanisms of *C. aeruginosa* against AGA. Finally, molecular docking was employed to verify the affinity between the components and targets.

2. Materials and Methods

2.1. Screening of Bioactive Compounds in C. aeruginosa

The Indian Medicinal Plants, Phytochemistry and Therapeutics 2.0 (IMPPAT 2.0) online database (https://cb.imsc.res.in/imppat/home (accessed on 31 January 2024) [16] was used in search of compounds present in *C. aeruginosa*. This database integrates the phytochemicals of Indian medicinal plants and their pharmacokinetic properties, including drug-likeness, blood–brain barrier permeation, gastrointestinal absorption, etc. Literature mining was also conducted for further collection. The physicochemical, drug-like, and pharmacokinetic parameters of the additional compounds were computed through SwissADME (http://www.swissadme.ch/ (accessed on 1 February 2024)) [17]. The compounds that met at least three drug-likeness principles and had high gastrointestinal absorption and an oral bioavailability greater than 30% were selected and classified as bioactive ones.

2.2. Target Gene Prediction in C. aeruginosa

The targets of the screened potentially bioactive compounds were determined through SwissTargetPrediction (http://www.swisstargetprediction.ch/ (accessed on 30 May 2024) [18], a web server that uses a combination of two-dimensional and three-dimensional similarity metrics with known ligands to reliably predict the protein targets of compounds. For the target genes prediction *C. aeruginosa*, the canonical SMILES of

compounds were copied to SwissTargetPrediction. "*Homo sapiens*" was selected as the study species to restrict the analysis of the target genes to those within humans, ensuring the relevance to human biology.

2.3. Target Gene Prediction in Androgenetic Alopecia

The GenCLip 3 (http://ci.smu.edu.cn/genclip3/analysis.php accessed on 30 May 2024) [19], DisGenNet (https://www.disgenet.org/ accessed on 30 May 2024) [20], Online Mendelian Inheritance in Man (OMIM) (https://omim.org/ accessed on 30 May 2024) [21], and GeneCards (https://www.genecards.org/ accessed on 30 May 2024) [22] databases were utilized to find human AGA-related targets using "androgenetic alopecia" as the keyword. The search results retrieved from the mentioned databases were combined, and duplicate targets were removed to acquire the potential target genes for treating AGA.

2.4. Protein–Protein Interaction Network

The target genes for the protein–protein interaction (PPI) network were obtained by determining the common targets of *C. aeruginosa* and AGA through a Venn diagram plotted in Venny 2.1 (https://bioinfogp.cnb.csic.es/tools/venny/ accessed on 30 May 2024). The PPI network of common targets was constructed by the Search Tool for Retrieval of Interacting Genes (STRING) (https://string-db.org/ accessed on 30 May 2024) [23], a database of predicted and known protein interactions, to investigate the relationship between the imported genes. The analysis was restricted to proteins found in "*Homo sapiens*" species. Afterward, the PPI network was imported into the Cytoscape (version 3.10.0) software for further analysis. CytoHubba, a Cytoscape plugin, was used to identify the potential hub target genes in the network. Three algorithms were employed—maximal clique centrality (MCC), maximum neighborhood component (MNC), and degree—to rank the best 10 genes based on the scores. The results were then intersected in which the overlapped genes represent the final set of hub targets. Moreover, MCODE was used for the cluster analysis of the PPI network with parameters set to default.

2.5. Gene Ontology and Pathway Enrichment Analysis

The gene ontology (GO) and Kyoto Encyclopedia of Genes and Genomes (KEGG) pathway enrichment analysis was performed to explore the biological mechanism underlying *C. aeruginosa* and its influence on AGA. GO is widely recognized for defining and describing genes from three aspects—biological process (BP), molecular function (MF), and cellular component (CC). KEGG, on the other hand, is a massive compilation of databases on drugs, genomes, enzymes, and biological pathways, among others. The enrichment analysis for the common targets was conducted using Metascape (https://metascape.org/gp/index.html accessed on 30 May 2024) [24], a gene annotation and analysis repository. Herein, the analysis was considered for "*Homo sapiens*" only, and p-value < 0.01 served as the cutoff. The results were taken as the top 20 based on descending $-\log10(p\text{-value})$. The results were visualized in the form of a bar chart with the help of the Scientific and Research plot tool (SRplot) (http://www.bioinformatics.com.cn/SRplot accessed on 30 May 2024).

2.6. Components–Targets–Pathways Network Construction

Cytoscape (version 3.10.0) was used to plot a network for the top 20 KEGG pathways with the corresponding potentially bioactive compounds and targets associated with them to effectively display the interactions between *C. aeruginosa* and AGA and ultimately characterize the therapeutic mechanisms of the former on the latter.

2.7. Molecular Docking

Molecular docking was applied to validate the binding between the core compounds of *C. aeruginosa* and the identified hub target genes. The crystal structures of human hub genes were downloaded from the RCSB Protein Data Bank (PDB) (https://www.rcsb.org/ accessed on 30 May 2024), while the 3D structures of the *C. aeruginosa* core compounds

were retrieved from the PubChem database (https://pubchem.ncbi.nlm.nih.gov/ accessed on 30 May 2024). The docking was performed using CB-Dock 2 (http://clab.labshare.co.uk/cb-dock/php/index.php accessed on 30 May 2024) [25], a protein–ligand blind docking tool that integrates the well-known molecular docking software Autodock Vina 1.1.2 to identify the binding site and predict binding pose.

3. Results

3.1. Bioactive Compounds in C. aeruginosa

Through IMPPAT, 93 compounds were found in the *C. aeruginosa* plant. Additionally, a literature search reveals a review article that described the phytochemical composition of *C. aeruginosa* [26], extracting 10 more compounds after eliminating the duplicates and those lacking structural information. In total, 103 compounds were screened, as shown in Table 1. However, only 66 were found to be bioactive after filtering with the parameters of an oral bioavailability greater than 30%, high gastrointestinal absorption, and adherence to three druglike rule-based filters, with one being the Lipinski rules. Interestingly, all compounds had bioavailability scores of 0.55, besides their high gastrointestinal absorption. A bioavailability score greater than 0.55 is assigned to any compound complying with Lipinski's rules and is considered ideal as it indicates the compound's optimal absorption [27].

Table 1. Bioactive compounds in *C. aeruginosa*.

No.	Compound	MW	OB	GIA	Drug-Likeness				
					Lipinski	Ghose	Veber	Muegge	Egan
1	Zedoarol	246.31	0.55	High	Yes	Yes	Yes	Yes	Yes
2	Myrcene *	136.24	0.55	Low	Yes	Yes	No	Yes	Yes
3	Trans-Tagetone	152.24	0.55	High	Yes	Yes	No	Yes	Yes
4	Furanodienone	230.31	0.55	High	Yes	Yes	Yes	Yes	Yes
5	gamma-Terpinene *	136.24	0.55	Low	Yes	Yes	No	Yes	Yes
6	1-Hexen-3-OL	100.16	0.55	High	Yes	Yes	No	Yes	Yes
7	p-Cymene *	134.22	0.55	Low	Yes	Yes	No	Yes	Yes
8	Curdione	236.36	0.55	High	Yes	Yes	Yes	Yes	Yes
9	Myrtenal	150.22	0.55	High	Yes	Yes	No	Yes	Yes
10	Germacrone	218.34	0.55	High	Yes	Yes	Yes	Yes	Yes
11	Isocurcumenol	234.34	0.55	High	Yes	Yes	Yes	Yes	Yes
12	1-Hexanol	102.18	0.55	High	Yes	Yes	No	Yes	Yes
13	beta-Cubebene *	204.36	0.55	Low	Yes	Yes	Yes	Yes	Yes
14	Eucalyptol	154.25	0.55	High	Yes	Yes	No	Yes	Yes
15	beta-Elemene *	204.36	0.55	Low	No	Yes	Yes	Yes	Yes
16	Furanogermenone	232.32	0.55	High	Yes	Yes	Yes	Yes	Yes
17	Curzerene	216.32	0.55	High	Yes	Yes	Yes	Yes	Yes
18	(+)-Curcumenol	234.34	0.55	High	Yes	Yes	Yes	Yes	Yes
19	4-Carvomenthenol	154.25	0.55	High	Yes	Yes	No	Yes	Yes
20	(1R)-2-methyl-5-propan-2-ylbicyclo[3.1.0]hex-2-ene *	136.24	0.55	Low	Yes	Yes	No	Yes	Yes
21	Curzerenone	230.31	0.55	High	Yes	Yes	Yes	Yes	Yes
22	alpha-Selinene *	204.36	0.55	Low	No	Yes	Yes	Yes	Yes
23	cis-3-Hexen-1-ol	100.16	0.55	High	Yes	Yes	No	Yes	Yes
24	d-Borneol	154.25	0.55	High	Yes	Yes	No	Yes	Yes
25	Terpinolene *	136.24	0.55	Low	Yes	Yes	No	Yes	Yes
26	beta-Farnesene *	204.36	0.55	Low	No	Yes	Yes	Yes	Yes
27	Curcumanolide B	234.34	0.55	High	Yes	Yes	Yes	Yes	Yes
28	Curcumanolides A	234.34	0.55	High	Yes	Yes	Yes	Yes	Yes
29	2-Hexen-1-OL	100.16	0.55	High	Yes	Yes	No	Yes	Yes
30	Humulene *	204.36	0.55	Low	No	Yes	Yes	Yes	Yes
31	Pulegone	152.24	0.55	High	Yes	Yes	No	Yes	Yes
32	Thujone	152.24	0.55	High	Yes	Yes	No	Yes	Yes
33	(+)-delta-Cadinene *	204.36	0.55	Low	No	Yes	Yes	Yes	Yes

Table 1. *Cont.*

No.	Compound	MW	OB	GIA	Drug-Likeness				
					Lipinski	Ghose	Veber	Muegge	Egan
34	(-)-cis-Carveol	152.24	0.55	High	Yes	Yes	No	Yes	Yes
35	Camphor	152.24	0.55	High	Yes	Yes	No	Yes	Yes
36	Linalool	154.25	0.55	High	Yes	Yes	No	Yes	Yes
37	alpha-Pinene *	136.24	0.55	Low	Yes	Yes	No	Yes	Yes
38	Carvone	150.22	0.55	High	Yes	Yes	No	Yes	Yes
39	beta-Pinene *	136.24	0.55	Low	Yes	Yes	No	Yes	Yes
40	alpha-Fenchol	154.25	0.55	High	Yes	Yes	No	Yes	Yes
41	alpha-Terpineol	154.25	0.55	High	Yes	Yes	No	Yes	Yes
42	Sabinene *	136.24	0.55	Low	Yes	Yes	No	Yes	Yes
43	trans-Pinocarveol	152.24	0.55	High	Yes	Yes	No	Yes	Yes
44	Caryophyllene oxide	220.36	0.55	High	Yes	Yes	Yes	Yes	Yes
45	Phytol *	296.54	0.55	Low	No	Yes	No	No	No
46	(Z)-beta-Ocimene *	136.24	0.55	Low	Yes	Yes	No	Yes	Yes
47	gamma-Elemene *	204.36	0.55	Low	No	Yes	Yes	Yes	Yes
48	beta-Selinene *	204.36	0.55	Low	No	Yes	Yes	Yes	Yes
49	beta-Caryophyllene *	204.36	0.55	Low	No	Yes	Yes	Yes	Yes
50	(E)-beta-ocimene *	136.24	0.55	Low	Yes	Yes	No	Yes	Yes
51	Camphene *	136.24	0.55	Low	Yes	Yes	No	Yes	Yes
52	Limonene *	136.24	0.55	Low	Yes	Yes	No	Yes	Yes
53	trans-Verbenol	152.24	0.55	High	Yes	Yes	No	Yes	Yes
54	Allo-Aromadendrene *	204.36	0.55	Low	Yes	Yes	Yes	Yes	Yes
55	2-Heptanol	116.2	0.55	High	Yes	Yes	No	Yes	Yes
56	Myrtenol	152.24	0.55	High	Yes	Yes	No	Yes	Yes
57	beta-Bisabolene *	204.36	0.55	Low	No	Yes	Yes	Yes	Yes
58	Curcumenone	234.43	0.55	High	Yes	Yes	Yes	Yes	Yes
59	2-Undecanol	172.31	0.55	High	Yes	Yes	Yes	Yes	Yes
60	gamma-Terpineol	154.24	0.55	High	Yes	Yes	No	Yes	Yes
61	Humuladienone	220.36	0.55	High	Yes	Yes	Yes	Yes	Yes
62	(-)-beta-Curcumene *	204.36	0.55	Low	No	Yes	Yes	Yes	Yes
63	Dehydrocurdione	234.43	0.55	High	Yes	Yes	Yes	Yes	Yes
64	Tetradecanal	212.38	0.55	High	Yes	Yes	No	Yes	Yes
65	Bisacumol	218.34	0.55	High	Yes	Yes	Yes	Yes	Yes
66	Tricyclene *	136.24	0.55	Low	Yes	Yes	No	Yes	Yes
67	Linalyl acetate	196.29	0.55	High	Yes	Yes	Yes	Yes	Yes
68	4′-Methylacetophenone	134.18	0.55	High	Yes	Yes	No	Yes	Yes
69	Xanthorrhizol	218.34	0.55	High	Yes	Yes	Yes	Yes	Yes
70	1-Methyl-4-(prop-1-en-2-yl)benzene *	132.21	0.55	Low	Yes	Yes	No	Yes	Yes
71	Linalyl isobutyrate	224.34	0.55	High	Yes	Yes	Yes	Yes	Yes
72	alpha-Guaiene *	204.36	0.55	Low	No	Yes	Yes	Yes	Yes
73	2-Nonanol	144.26	0.55	High	Yes	Yes	No	Yes	Yes
74	2-Nonanone	142.24	0.55	High	Yes	Yes	No	Yes	Yes
75	3,7(11)-Eudesmadiene *	204.46	0.55	Low	No	Yes	Yes	Yes	Yes
76	Camphene hydrate	154.25	0.55	High	Yes	Yes	No	Yes	Yes
78	Curcuphenol	218.34	0.55	High	Yes	Yes	Yes	Yes	Yes
79	Turmerol	220.36	0.55	High	Yes	Yes	Yes	Yes	Yes
80	2-Undecanone	170.3	0.55	High	Yes	Yes	Yes	Yes	Yes
81	beta-Eudesmol	222.37	0.55	High	Yes	Yes	Yes	Yes	Yes
82	Farnesol	222.37	0.55	High	Yes	Yes	Yes	Yes	Yes
83	alpha-Terpinene *	136.23	0.55	Low	Yes	Yes	No	Yes	Yes
84	cis-beta-Farnesene *	204.36	0.55	Low	No	Yes	Yes	Yes	Yes
85	Zingiberene *	204.36	0.55	Low	No	Yes	Yes	Yes	Yes
86	(+)-beta-Phellandrene *	136.23	0.55	Low	Yes	Yes	No	Yes	Yes
87	alpha-Curcumene *	202.34	0.55	Low	No	Yes	Yes	Yes	Yes
88	ar-Turmerone	216.32	0.55	High	Yes	Yes	Yes	Yes	Yes

Table 1. *Cont.*

No.	Compound	MW	OB	GIA	Drug-Likeness				
					Lipinski	Ghose	Veber	Muegge	Egan
89	3-(1,5-Dimethyl-4-hexenyl)-6-methylene-1-cyclohexene *	204.36	0.55	Low	Yes	Yes	No	Yes	Yes
90	Linalool oxide B	170.25	0.55	High	Yes	Yes	Yes	Yes	Yes
91	delta-Elemene *	204.36	0.55	Low	No	Yes	Yes	Yes	Yes
92	alpha-Atlantone	218.34	0.55	High	Yes	Yes	Yes	Yes	Yes
93	alpha-Phellandrene *	136.24	0.55	Low	Yes	Yes	No	Yes	Yes
94	Nerolidol	222.37	0.55	High	Yes	Yes	Yes	Yes	Yes
95	Flavone	222.24	0.55	High	Yes	Yes	Yes	Yes	Yes
96	Zedoalactone A	266.36	0.55	High	Yes	Yes	Yes	Yes	Yes
97	Zedoarondiol	252.35	0.55	High	Yes	Yes	Yes	Yes	Yes
98	Furanodiene	216.32	0.55	High	Yes	Yes	Yes	Yes	Yes
99	Zederone	246.30	0.55	High	Yes	Yes	Yes	Yes	Yes
100	Pyrocurzerenone	212.29	0.55	High	Yes	Yes	Yes	Yes	Yes
101	Dehydrochromolaenin	210.27	0.55	High	Yes	Yes	Yes	Yes	Yes
102	Isoaromadendrene epoxide	220.35	0.55	High	Yes	Yes	Yes	Yes	Yes
103	Demethoxycurcumin	338.35	0.55	High	No	Yes	Yes	Yes	Yes

* Did not meet the screening conditions.

3.2. Predicted Target Genes of *C. aeruginosa* and AGA

The 66 druglike compounds of *C. aeruginosa* had their target genes predicted through SwissTargetPrediction, yielding 795 human proteins after removing the duplicates (Supplementary Table S1). On the other hand, a total of 672 genes related to AGA were collected, of which 100 genes were from GenClip, 112 from DisGeNet, 452 from GeneCard, and 8 from OMIM. After the deletion of duplicates, 562 potential AGA-related targets were obtained (Supplementary Table S2).

3.3. Common Targets of *C. aeruginosa* and AGA

The intersection of potential *C. aeruginosa* target genes and AGA-related genes revealed 59 overlapping genes, as presented by the Venn diagram shown in Figure 1. The overlapped genes, as listed in Table A1 (see Appendix A), indicate the potential targets of *C. aeruginosa* for the therapy of AGA. They were collected for further mechanisms study of the former against the latter.

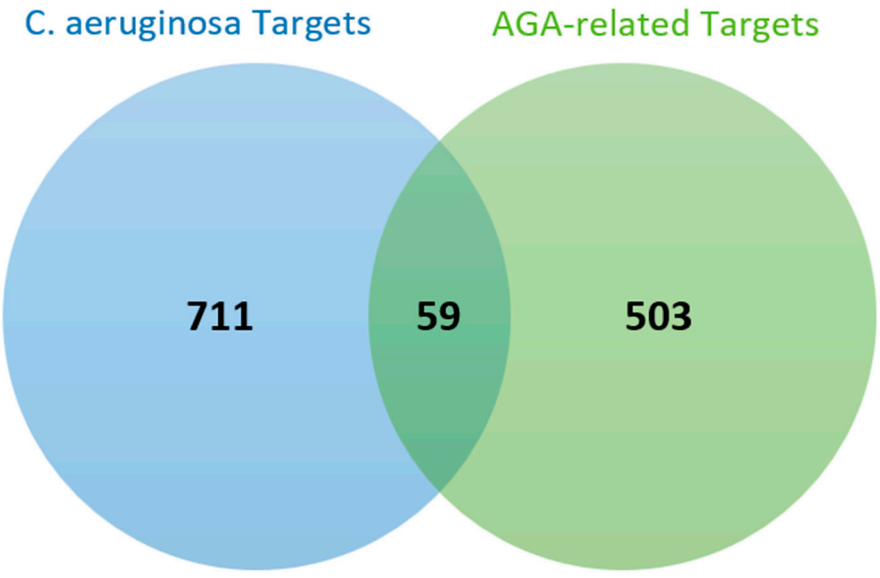


Figure 1. The 59 overlapping targets between *C. aeruginosa* and AGA identified by Venn diagram.

3.4. Protein–Protein Interaction (PPI) Network

The 59 targets associated with AGA and determined as targets for *C. aeruginosa* bioactive compounds were imported to STRING to construct a PPI network and analyze the relationship between them. An original PPI network comprising 59 nodes, of which one was disconnected, and 449 edges with an average node degree of 15.2 were produced, as shown in Figure 2. Also, it had an average local clustering coefficient of 0.629, indicating how connected the nodes were. The expected number of edges was 178, which was much lesser than the actual edges of the network, and the PPI enrichment *p*-value was observed to be $<1.0 \times 10^{-16}$. Hence, the network had significantly greater interactions than expected for the random network of similar size, and the proteins, represented by nodes, were at least partially biologically connected as a cluster.



Figure 2. Original PPI network of 59 potential targets of *C. aeruginosa* in AGA constructed by STRING.

Subsequently, the original PPI network from STRING was reconstructed in Cytoscape for visualization and further analysis. The reconstructed network, as shown in Figure 3, contained 58 nodes and 449 edges while removing one unconnected gene. The color of the node differed depending on its degree value, with darker colors reflecting greater

values. The larger the degree, the more the involvement of biological functions, suggesting protein's vital role in the network. Thus, the nodes with darker colors may serve as essential targets for the therapeutic effects of *C. aeruginosa* in AGA.

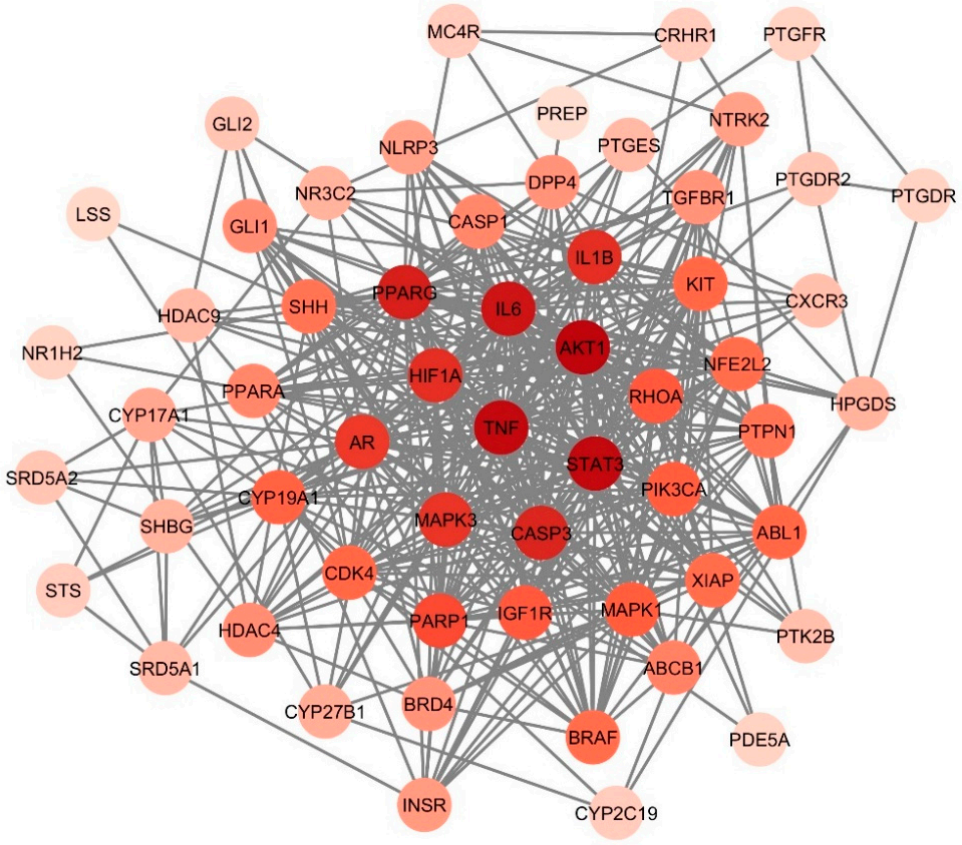


Figure 3. The PPI network (58 nodes and 449 edges) showing the degree of the targets reconstructed by Cytoscape 3.10.2. The darker the color of the node, the greater its degree.

3.5. Identification of Hub Genes

To determine the hub targets, the CytoHubba plug-in of Cytoscape 3.10.2 was used to analyze each node by incorporating three topological algorithms, namely, maximal clique centrality (MCC), maximum neighborhood component (MNC), and degree. Figure 4 shows the top 10 genes predicted by each algorithm based on their scores. Eight genes (CASP3, AKT1, AR, IL6, PPARG, STAT3, HIF1A, and MAPK3) were screened out after intersecting the three results, as revealed in Figure 4D. These highly connected genes, as shown in Figure 4E, represent the hub target genes of *C. aeruginosa* in AGA treatment.

3.6. Cluster Analysis of PPI Network

MCODE plug-in was employed for cluster analysis of the PPI, yielding three cluster modules, as shown in Figure 5. Module 1 possessed 23 nodes and 186 edges; Module 2 comprised 6 nodes and 11 edges; and Module 3 comprised 3 nodes and 3 edges. Module 1 had the highest average score of 16.91, followed by Module 2 and Module 3, whose scores were 4.40 and 3.00, respectively. In the PPI network, modules with greater average scores may have more significant roles. Hence, Module 1 was the most important. Consequently, all identified hub genes were clustered in this module.

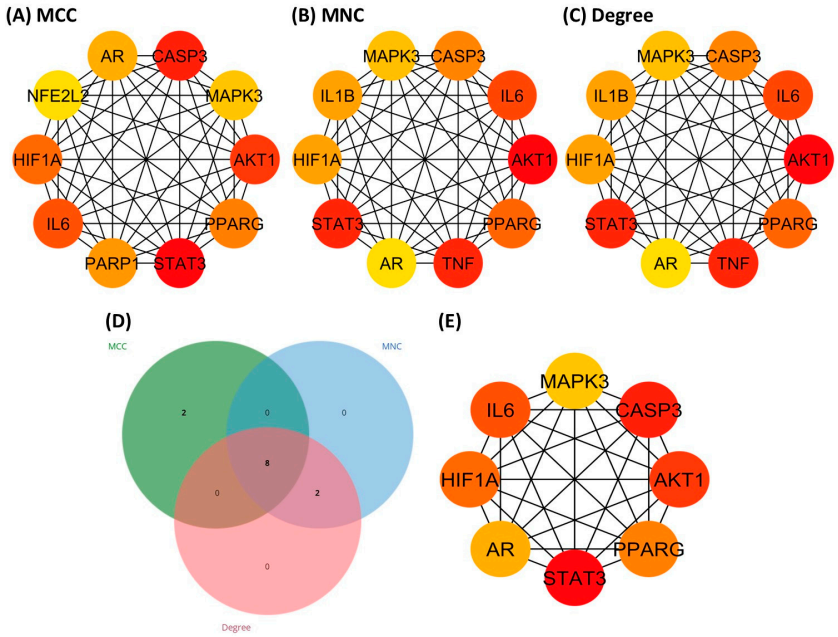


Figure 4. The top 10 hub gene networks of *C. aeruginosa* bioactive compounds against AGA from the employment of (**A**) maximal clique centrality, (**B**) maximum neighborhood component (MNC), and (**C**) degree. The warmer the color, the higher the score. The score correlates with the rank of genes in the network. (**D**) The Venn diagram intersecting the results of the three algorithms, revealing eight hub genes. (**E**) The PPI network of eight hub genes. Node color denotes interaction degree (red for high degree, orange for intermediate degree, and yellow for low degree).

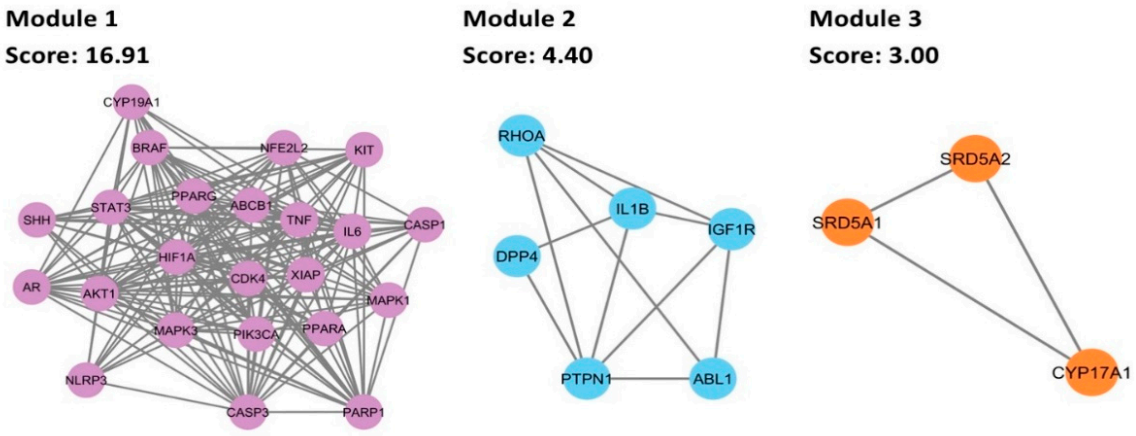


Figure 5. The modules obtained from the cluster analysis of the PPI network.

3.7. GO and KEGG Enrichment Analyses

GO and KEGG enrichment analyses of the 59 common targets in Metascape yielded 1055 biological processes, 64 molecular functions, 36 cellular components, and 150 KEGG pathway terms, wherein the top 20 terms in each category are visualized in Figure 6 and listed in Tables A2–A4 (see Appendix A). Based on biological processes, the function of the bioactive compounds is mostly concentrated on response to peptides, lipids, and hormones, among others, suggesting that *C. aeruginosa* can modulate the hormones participating in AGA. Additionally, the majority of the genes are coded for protein in the receptor complex, transcription regulator complex, and plasma membrane protein complex, suggesting that *C. aeruginosa* targets protein complexes. Also, the cellular components included the cell body, which may indicate the potential interactions of *C. aeruginosa* bioactive compounds with cells relevant to the hair growth cycle. Molecularly, the functions of *C. aeruginosa*

were mainly enriched in the activity of and binding to protein kinase and transcription factors, as well as hormone binding and nuclear receptor activity. This indicated that *C. aeruginosa* affects these proteins, which are the categories of the identified AGA-related targets of *C. aeruginosa.* Lastly, The KEGG enrichment showed the potential signaling pathways by which *C. aeruginosa* played an anti-AGA role, including MAPK and HIF-1 signaling pathways.

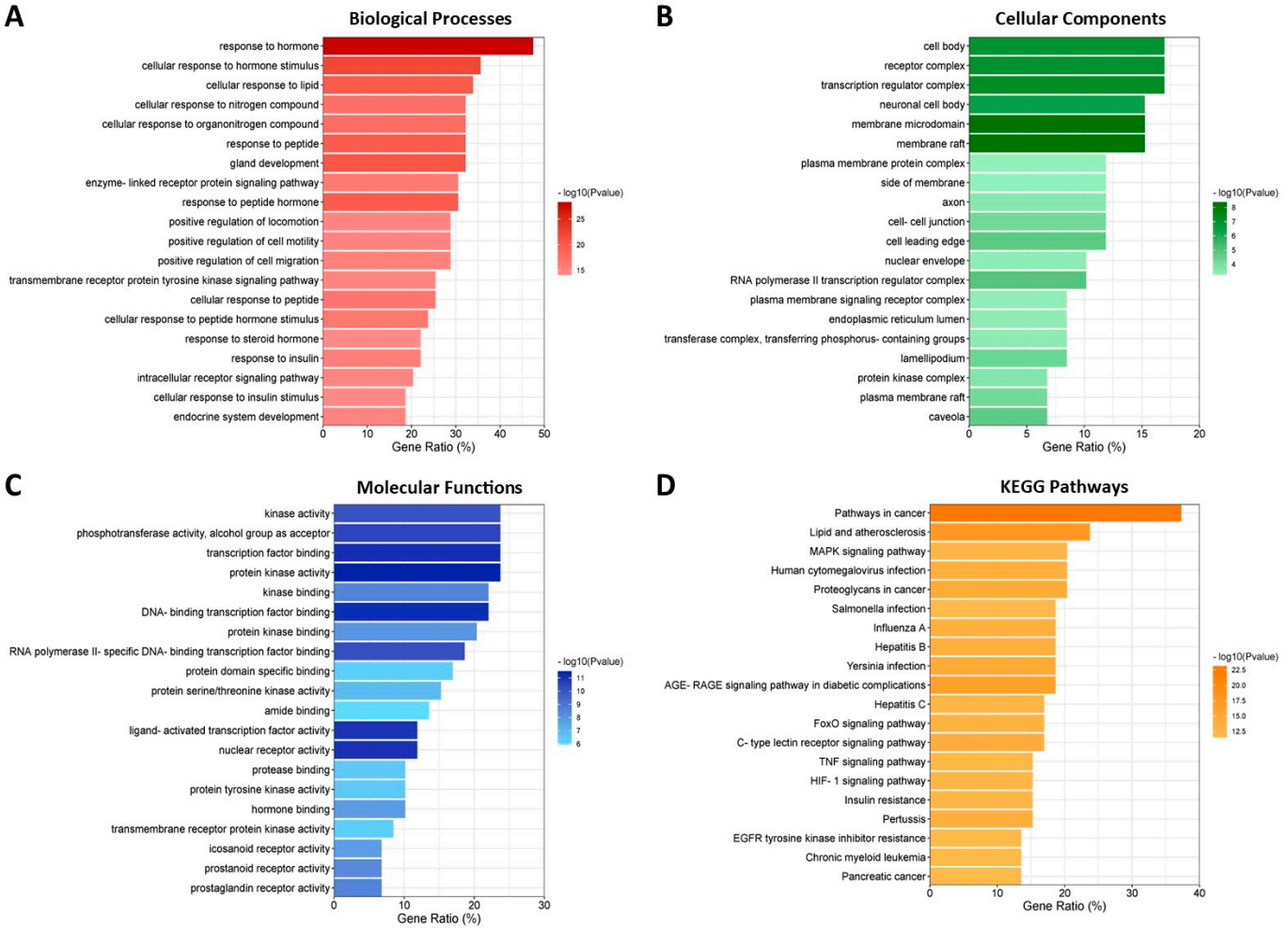


Figure 6. Enrichment analyses of *C. aeruginosa* potential targets in AGA for the top 20 GO annotations and KEGG pathways: (**A**) GO biological processes, (**B**) GO cellular components, (**C**) GO molecular functions, and (**D**) KEGG pathways.

3.8. Components–Targets–Pathways Network

A network representation of the interaction between *C. aeruginosa* bioactive compounds, its potential target genes linked to AGA, and pathways associated with the targets was constructed through Cytoscape and portrayed as the components–targets–pathways network shown in Figure 7. The compounds, targets, and pathways were represented by yellow elliptical nodes, blue round rectangular nodes, and red arrow-shaped nodes, respectively. The network contained 144 nodes (66 compounds, 58 target genes, and 20 pathways) and 847 edges, showing the intricate relationships between them. Topological analysis of the components–targets network revealed trans-verbenol, myrtenal, carvone, alpha-atlantone, and isoaromandendrene epoxide as core components, exhibiting degrees of 16, 15, 15, 14, and 14, respectively, which were the highest among the compounds. Generally, this network revealed the multi-components of *C. aeruginosa* exerting synergistic multi-targeted effects against AGA.

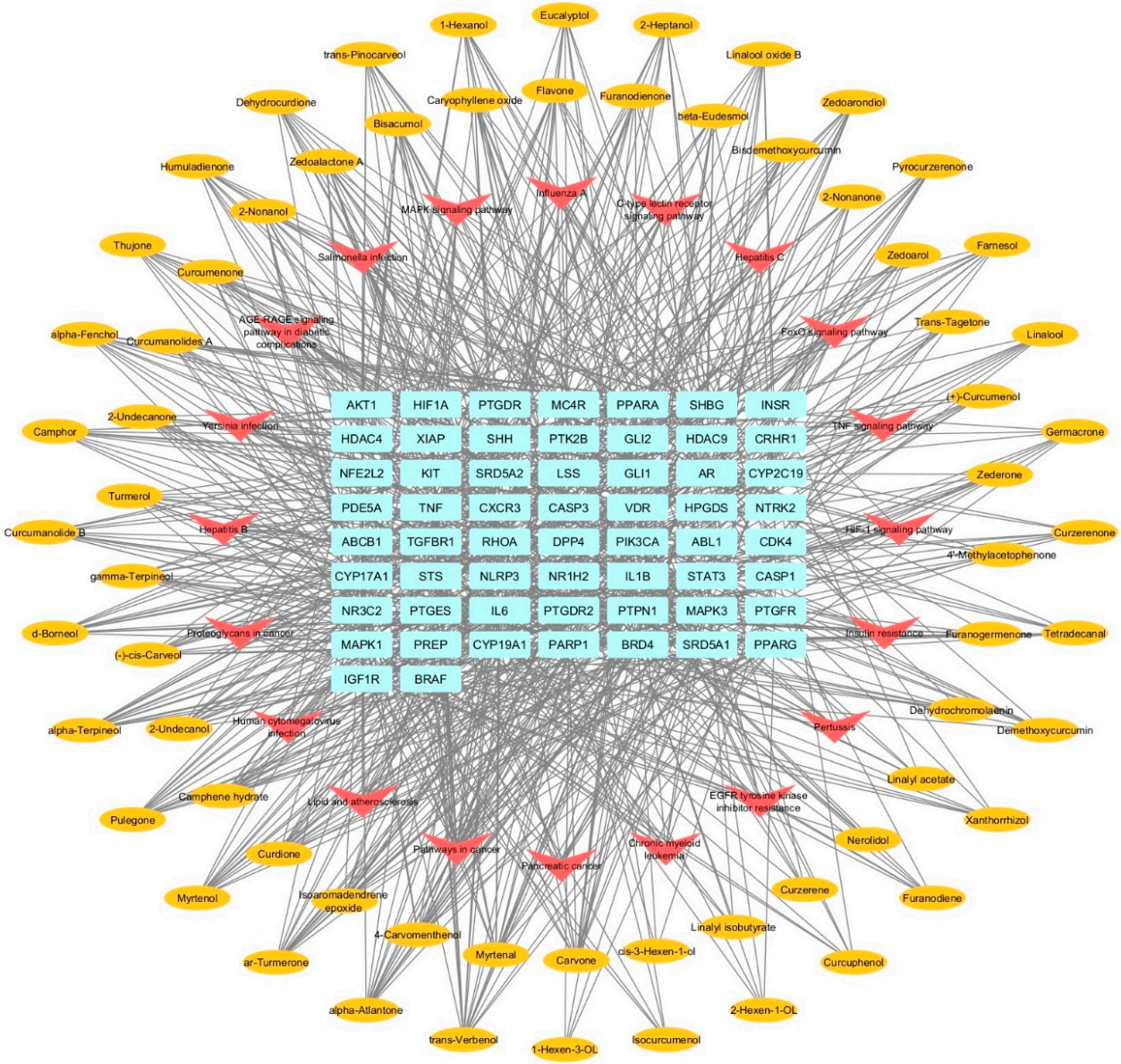


Figure 7. The components–targets–pathways network displaying the potential mechanism of *C. aeruginosa* against AGA (yellow ellipses: compounds; red arrows: pathways; blue rectangles: targets).

3.9. Molecular Docking

The hub target genes (CASP3, AKT1, AR, IL6, PPARG, STAT3, HIF1A, and MAPK3) were molecularly docked with the core components to ascertain whether the core components (trans-verbenol, myrtenal, carvone, alpha-atlantone, and isoaromandendrene epoxide) of *C. aeruginosa* could bind to the protein targets predicted by SwissTargetPrediction. Two positive controls were also docked, namely, finasteride and minoxidil. Generally, the binding energy between the ligand compounds and receptor proteins dictates their structural stability. The lower the binding energy, the greater the affinity between the protein target and component. Based on the molecular docking studies, as shown in Figure 8, the binding energy between the core compounds and hub genes ranged from −4.6 to −8.9 kcal/mol. The results showed that the binding energies were less than 0, suggesting they spontaneously bound to one another. Binding energies less than −5 kcal/mol are believed to create more stable structures as opposed to those with greater binding energies. Hence, all molecules could bind stably to the target genes with strong affinity except for carvone and myrtenal when bound to HIF1A. AKT1 and AR, among the target genes, had

the highest binding affinity with the core compounds. This may imply that targeting these proteins plays an essential role in AGA treatment by *C. aeruginosa* bioactive compounds. Strikingly, alpha-atlantone and isoaromandendrene epoxide demonstrated superior affinity to AR when compared to controls. The top four stable ligand-receptor complexes were selected for visualization, as shown in Figure 9, and their binding sites were tabulated in Table 2. Since both alpha-atlantone and isoaromandendrene epoxide are sesquiterpenes, they are bound to similar amino acid residue sites in the AKT1 complex.

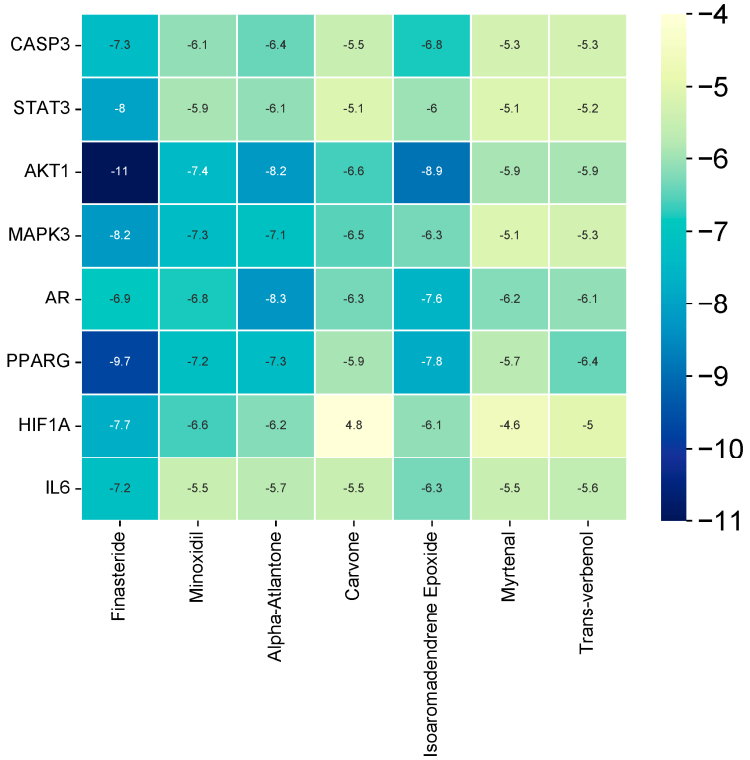


Figure 8. Heatmap of the molecular docking of *C. aeruginosa* core compounds with hub target genes. The bluer the color, the greater the binding energy and binding affinity between the ligand and the receptor.

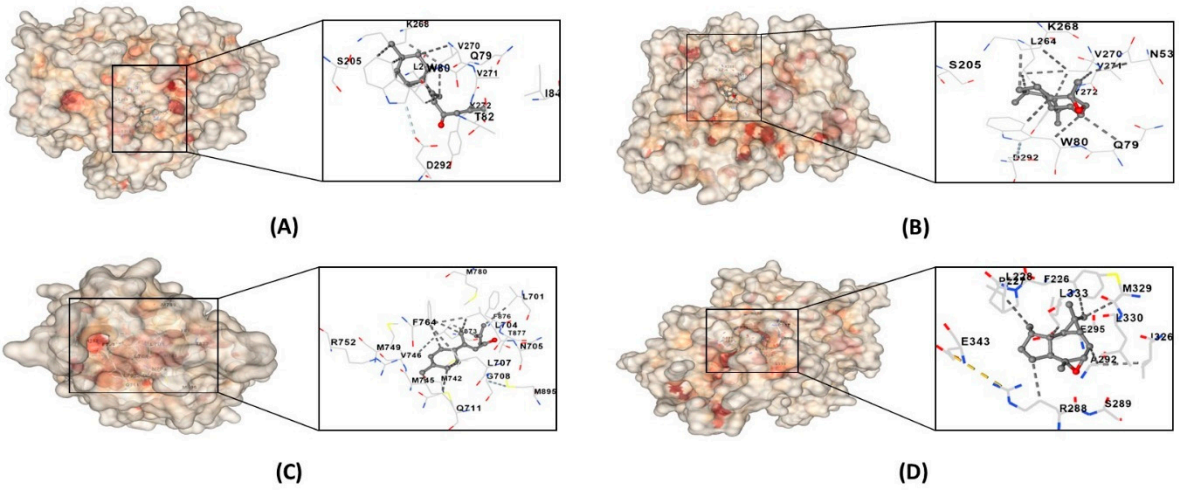


Figure 9. The top four ligand-receptor complexes: (**A**) AKT1-alpha-atlantone, (**B**) AKT1-isoaromandendrene epoxide, (**C**) AR-alpha-atlantone, and (**D**) PPARG- isoaromandendrene epoxide.

Table 2. Binding site interactions of top 4 ligand–protein complexes.

Compound	Protein	Binding Sites
alpha-atlantone	AR	Leu701, Leu704, Asn705, Leu707, Gly708, Gln711, Trp741, Met742, Met745, Val746, Met749, Arg752, Phe764, Met780, Met787, Leu873, Phe876, THR877 Leu880, Phe891, Met895, Ile899
	AKT1	Asn53, Asn54, Ala58, Gln59, Leu78, Gln79, Trp80, Thr82, Ile84, Asn199, Val201, Ser205, Leu210, Thr211, Leu264, Lys268, Val270, Val271, Tyr272, Ile290, Thr291, Asp292
isoaromandendrene epoxide	AKT1	Glu17, Tyr18, Asn53, Asn54, Ser56, Ala58, Gln59, Gln79, Trp80, Thr81, Thr82, Ile84, Glu85, Arg86, Lys179, Val201, Ser205, Leu210, Thr211, Leu213, Tyr263, Leu264, Lys268, Val270, Val271, Tyr272, Arg273, Asp274, Asn279, Thr291, Asp292, Phe293, Gly294, Cys296, Lys297, Glu298, Tyr326
	PPARG	Phe226, Pro227, Leu228, Gly284, Cys285, Arg288, Ser289, Glu291, Ala292 Glu295, Ile296, Ile325, Ile326, Met329, Leu330, Leu333, Val339, Leu340, Ile341, Ser342, Glu343, Gly344, Met364

4. Discussion

AGA is a multifactorial hair loss disorder, and those suffering from this disease have limited options for medical treatment. Drugs like finasteride and minoxidil cause side effects, restricting their long-term administration. Moreover, invasive treatments like hair transplantation and platelet-rich plasma (PRP) require repeated procedures, resulting in costly investments [28,29]. Currently, topical herbal preparations are becoming more commonly available due to their greater compliance rate, broader active spectrum, more affordable price, and lesser side effects [30,31]. Thus, they are anticipated to be extensively utilized for AGA complementary and alternative medicine. *C. aeruginosa*, as a topical preparation, has been shown to exhibit anti-androgenic and hair growth effects due to its phytochemical content that may target different pathways involved in AGA. Accordingly, network pharmacology fits as a valid method for elucidating its multicomponent–multitarget anti-AGA mechanism.

The network pharmacology results revealed five compounds—trans-verbenol, myrtenal, carvone, alpha-atlantone, and isoaromandendrene epoxide—that might be the core components in *C. aeruginosa* and enable it to induce therapeutic effects against AGA. However, no studies reported their anti-androgenic and trichogenic effects yet, recommending further in vivo and in vitro studies to test their anti-AGA potential. Molecular docking analysis confirmed that the core components bound with the eight hub genes—CASP3, AKT1, AR, IL6, PPARG, STAT3, HIF1A, and MAPK3—implying potential interactions and modulation of these genes to treat AGA.

CASP3, whose role is central in executing cell apoptosis, is overexpressed in the bald area of AGA patients in the early courses of the disease, revealing the presence of inflammation and apoptosis at such stages [32]. Activation of CASP3 inhibits the PI3K/AKT signaling pathway, which mediates extracellular signals and intracellular responses and is critically involved in the regulation of cell proliferation, growth, and differentiation. This, in turn, stops hair follicles from transitioning from the resting phase to the anagen phase, blocks cell proliferation, promotes apoptosis, and finally degenerates hair follicles [33]. As such, inhibiting CASP3 activation helps reverse hair follicles' entry to the abnormal and degenerative anagen phases and stimulates hair growth.

Likewise, AKT1, one of the relevant serine/threonine protein kinases, regulates cell apoptosis and proliferation and serves as the main downstream molecule of the PI3K/AKT pathway, whose role is necessary for de novo hair follicle regeneration [34]. In response to extracellular signals, AKT1 can either act as a positive or negative regulator of the PI3K/AKT pathway via PIK3, leading to AR expression regulation [35].

AR-bound DHT is the main cause of AGA, with DHT-AR signaling strongly associated with AGA pathogenesis [36–38]. AR is primarily expressed in hair follicles, particularly dermal papilla cells (DPCs) [39]. When DHT binds to AGA, expression of growth inhibition

factors (i.e., DKK-1, TGF-β, and IL-6) is triggered [40,41]. IL-6 suppresses hair shaft elongation by inhibiting matrix cell proliferation and, thereby, stimulates hair follicle regression [42]. Additionally, PPARG also discourages hair growth, but by promoting mitochondrial activity [43]. Essentially, DHT-AR signaling facilitates the miniaturization of hair follicles, resulting in the apoptosis of keratinocytes [44] and DPCs [45] and, eventually, AGA progression. Therefore, treatment for AGA may benefit most from inhibiting AR expression due to the major role of AR in AGA.

Contrary to the alopecia-inducing effects of the earlier hub genes, STAT3, HIF1A, and MAPK3 are reported to counteract hair loss. STAT3 is required in the hair cycle during the onset of anagen because it activates keratinocytes for the continuation of the hair cycle [46]. Loss of STAT3 functions in keratinocytes increases apoptotic hair follicle stem cells (HFSCs), impairing the hair cycle process [47]. Contrastingly, gain of function raises progenitor cells and HFSCs above the bulge region, ensuring proper maintenance and growth of hair follicles [48]. With this, STAT3 regulation is critical in maintaining hair cycling and growth. Meanwhile, HIF1A regulates trichogenic gene expression in DPCs [49], suggesting a similar function to minoxidil, which exerts trichogenic effects ascribed by its vasodilating properties [50]. Lastly, MAPK's role in regenerating HFSCs, inducing anagen hair cycle, and modulating root hair tip growth is important in hair growth stimulation [51,52]. Specifically, when MAPK3 was upregulated, hair growth improved [53].

The GO enrichment analysis suggested that *C. aeruginosa* may regulate hormones, such as androgen, estrogen, and cortisol. Androgens, like testosterone and DHT, activate AR signaling, upregulating genes involved in hair growth suppression resulting from growth inhibition factors, vascular regression around dermal papilla [54], apoptosis [55], and DPC aging [56]. On the other hand, estrogen maintains hair follicle cycling [57], encourages healthy hair growth by activating the Wnt/β-catenin signaling pathway to sustain HFSC differentiation and proliferation [58,59], and shields hair follicles from oxidative stress and eventually hair follicle aging by modulating antioxidant enzymes [60]. Lastly, corticosterone, the cortisol counterpart in mice and the main stress hormone, disallows the entry of HFSCs into the anagen phase [61]. Thus, chronic stress can quicken hair aging and loss by influencing HFSC.

On the other hand, the KEGG enrichment showed the potential signaling pathways by which *C. aeruginosa* played an anti-AGA role, including MAPK and HIF-1 signaling pathways. The identified hub genes were implicated in the MAPK pathway (AKT1, CASP3, and MAPK3) and the HIF-1 pathway (AKT1, GIF1A, IL6, MAPK3, and STAT3) through which core compounds may act to modulate them. The combined effects of the compounds through their regulation of MAPK and HIF-1 pathways, together with direct interaction with other hub genes, create a synergistic approach to address various aspects of AGA pathogenesis. MAPK pathway is important in regulating normal cell survival, migration, proliferation, and migration [62]. In hair, MAPK has been revealed to amplify growth factor production [63], regulate the hair cycle and quiescence of HFSC [51], and promote HFSC differentiation and proliferation [64], thereby influencing hair follicle morphogenesis and regeneration. Currently, four MAPK signal transduction pathways are known in mammalian cells: extracellular signal-regulated kinases (ERKs) which stimulate DPC proliferation and anagen phase [65,66]; and p38 MAPKs and Jun N-terminal kinases (JNKs), both of which control Wnt/β-catenin pathway [67,68], the master regulator of hair cells.

Whereas the HIF-1 pathway has been shown to govern hair regeneration, regulating the size and shape of dermal papilla [69,70]. AGA has been associated with insufficient nutrient supply and reduced blood vessels. Consequently, HIF stimulation can come into play in this by regulating neovascularization and regeneration as DPCs react to hypoxia [71]. The HIF-1 pathway is strongly linked to the mechanism of action of minoxidil attributed to its vasodilating properties [72]. Clinical trials showed that the combination of minoxidil and *C. aeruginosa* stimulated hair growth more effectively than minoxidil alone [12,13]. The topical application of *C. aeruginosa* complimented minoxidil as it increased hair growth and decreased hair shedding by enhancing penetration [12,13]. This may be caused by *C.*

aeruginosa's potential regulation of the HIF-1 pathway, which is said to increase vasodilation, promoting conducive conditions for hair growth. Figure 10 shows the potential mechanism of *C. aeruginosa* against AGA. It is essential to consider that although MAPK and HIF-1 pathways influence AGA, their roles are part of a complex cascade of events rather than a direct one.

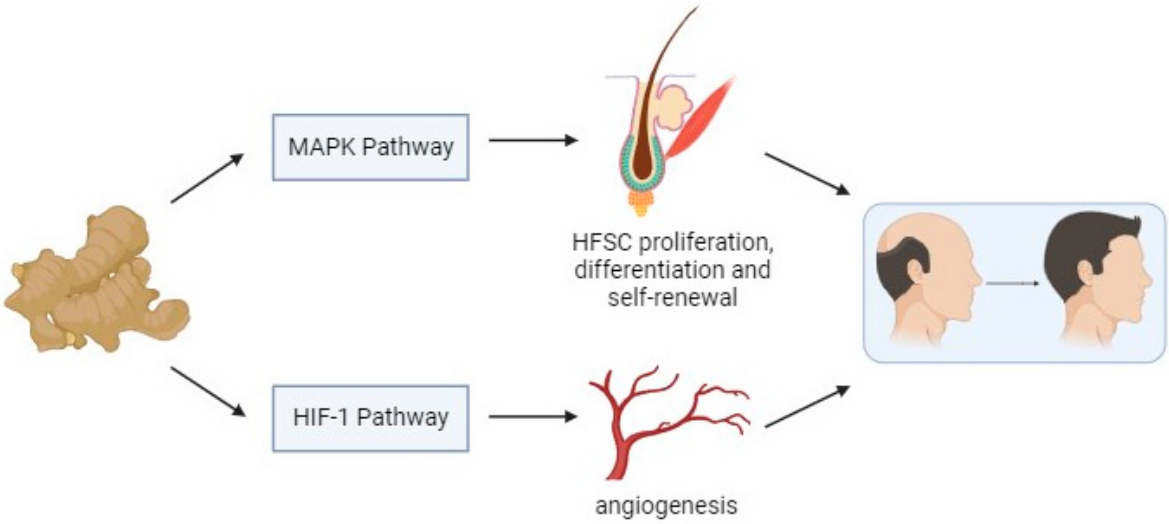


Figure 10. The potential mechanism of *Curcuma aeruginosa* Roxb. against androgenetic alopecia. Collectively, in the treatment of AGA, the MAPK pathway promotes hair follicle proliferation, differentiation, and self-renewal to maintain the hair cycle, and the HIF-1 pathway improves hair vascularization and nutrient supply conducive to hair growth.

Notably, Module 3 derived from the cluster analysis of the PPI network contained SRD5A2, SRD5A1, and CYP17A1, which are involved in androgen biosynthesis. SRD5As amplify DHT production in hair follicles of the scalp, causing AGA [73]. To date, steroidal drugs finasteride and dutasteride are used to treat AGA by acting as SRD5A inhibitors. Finasteride selectively inhibits SRD5A2 while dutasteride inhibits both SRD5A1 and SRD5A2. Accordingly, a prior study suggested that the potential mechanism of C. aeruginosa for its anti-androgenic effect is SRD5A inhibition [11]. Its sesquiterpene content, specifically germacrone, was on par with finasteride when it came to exhibiting anti-androgenic activity. It inhibited SRD5A to a similar extent as finasteride in suppressing the growth of testosterone-induced growth of human prostate cancer cells (in vitro) and hamster flank gland model (in vivo), thereby suggesting *C. aeruginosa* as a novel SRD5A inhibitor. Similarly, CYP17A1 is needed in DHT production, both in anterior and posterior routes [74,75]. Minoxidil suppresses CYP17A1 to inhibit AGA [76]. Therefore, synergizing this with MAPK and HIF-1 pathways may influence both anti-androgenic activities and hair growth effects, promoting healthy hair follicles and eventually preventing AGA.

While AGA affects both men and women, men are more commonly and severely impacted because of innate higher levels of androgens. Although *C. aeruginosa* exhibited trichogenic activities that could impact women too, men with genetic predispositions to AGA are likely to see more significant benefits from *C. aeruginosa* given its anti-androgenic effects. Additionally, younger men, whose AGA symptoms are not yet more pronounced, may experience greater advantages from early intervention using it to potentially prevent AGA. Further research is recommended to fully comprehend these effects across different patient populations. In terms of safety, no side effects were reported on the topical application of *C. aeruginosa* in clinical trials [12,13], as opposed to those associated with finasteride and minoxidil, namely, sexual dysfunction and dermatological problems. This underscores the potential of *C. aeruginosa* as an AGA treatment, warranting further investigation.

5. Conclusions

In summary, this study combined network pharmacology and molecular docking to elucidate the active compounds, putative targets, and potential mechanisms of *C. aeruginosa* in the treatment of AGA. The results pinpointed that bioactive compounds in *C. aeruginosa*, such as trans-verbenol, myrtenal, carvone, alpha-atlantone, and isoaromandendrene epoxide, may play a crucial role in AGA by eliciting their effects on key target genes, including CASP3, AKT1, AR, IL6, PPARG, STAT3, HIF1A, and MAPK3. The molecular docking studies indicated that these bioactive components of *C. aeruginosa* could effectively act on these targets. Also, enrichment analyses revealed that *C. aeruginosa* may play its therapeutic role against AGA by modulating both HIF-1 and MAPK pathways, offering new approaches in the treatment and prevention of AGA. Substantially, the findings showed that *C. aeruginosa* could treat AGA via a mechanism involving multiple components, targets, and pathways. Hence, the valuable results may imply that *C. aeruginosa* could be a promising option in developing new drugs for AGA. As bound by the limitations of bioinformatics data and in silico network pharmacology and molecular docking analysis, however, experimental exploration and further confirmation via in vivo and in vitro studies are recommended to verify the findings of this study.

Supplementary Materials: The following supporting information can be downloaded at https://www.mdpi.com/article/10.3390/biology13070497/s1, Table S1: Curcuma aeruginosa targets; Table S2: AGA-related targets.

Author Contributions: Conceptualization, A.M.L.S. and H.S.C.; methodology, A.M.L.S. and H.S.C.; software, A.M.L.S.; validation, A.M.L.S. and H.S.C.; formal analysis, A.M.L.S.; investigation, A.M.L.S.; resources, A.M.L.S.; data curation, A.M.L.S.; writing—original draft preparation, A.M.L.S.; writing—review and editing, A.M.L.S.; visualization, A.M.L.S.; supervision, H.S.C.; project administration, H.S.C.; funding acquisition, H.S.C. All authors have read and agreed to the published version of the manuscript.

Funding: This research received no external funding.

Institutional Review Board Statement: Not applicable.

Informed Consent Statement: Not applicable.

Data Availability Statement: The data and results presented in this study are available upon request from the first and corresponding author.

Conflicts of Interest: The authors declare no conflicts of interest.

Appendix A

Table A1. The common targets of *C. aeruginosa* and AGA.

No.	Gene	Full Name
1	PIK3CA	phosphatidylinositol-4,5-bisphosphate 3-kinase catalytic subunit alpha
2	CASP1	caspase 1
3	CYP2C19	cytochrome P450 family 2 subfamily C member 19
4	AR	androgen receptor
5	NR3C2	nuclear receptor subfamily 3 group C member 2
6	IGF1R	insulin-like growth factor 1 receptor
7	PARP1	poly (ADP-ribose) polymerase 1
8	KCNE1	potassium voltage-gated channel subfamily E regulatory subunit 1
9	VDR	vitamin D receptor
10	MAPK1	mitogen-activated protein kinase 1
11	CYP19A1	cytochrome P450 family 19 subfamily A member 1
12	PREP	prolyl endopeptidase
13	SRD5A1	steroid 5 alpha-reductase 1
14	HPGDS	hematopoietic prostaglandin D synthase
15	MC4R	melanocortin 4 receptor

Table A1. *Cont.*

No.	Gene	Full Name
16	CASP3	caspase 3
17	NLRP3	NLR family pyrin domain containing 3
18	BRD4	bromodomain containing 4
19	CYP17A1	cytochrome P450 family 17 subfamily A member 1
20	PTGES	prostaglandin E synthase
21	MAPK3	mitogen-activated protein kinase 3
22	SHBG	sex-hormone-binding globulin
23	SRD5A2	steroid 5 alpha-reductase 2
24	PPARG	peroxisome proliferator-activated receptor gamma
25	PPARA	peroxisome proliferator-activated receptor alpha
26	PTPN1	protein tyrosine phosphatase non-receptor type 1
27	IL6	interleukin 6
28	PTK2B	protein tyrosine kinase 2 beta
29	PDE5A	phosphodiesterase 5A
30	GLI2	GLI family zinc finger 2
31	GLI1	GLI family zinc finger 1
32	SHH	sonic hedgehog signaling molecule
33	DPP4	dipeptidyl peptidase 4
34	HIF1A	hypoxia-inducible factor 1 subunit alpha
35	NR1H2	nuclear receptor subfamily 1 group H member 2
36	PTGFR	prostaglandin F receptor
37	PTGDR	prostaglandin D2 receptor
38	TGFBR1	transforming growth factor beta receptor 1
39	IL1B	interleukin 1 beta
40	CRHR1	corticotropin-releasing hormone receptor 1
41	LSS	lanosterol synthase
42	TNF	tumor necrosis factor
43	CDK4	cyclin-dependent kinase 4
44	AKT1	AKT serine/threonine kinase 1
45	CXCR3	C-X-C motif chemokine receptor 3
46	KIT	KIT proto-oncogene receptor tyrosine kinase
47	RHOA	ras homolog family member A
48	ABCB1	ATP-binding cassette subfamily B member 1
49	BRAF	B-Raf proto-oncogene, serine/threonine kinase
50	STAT3	signal transducer and activator of transcription 3
51	PTGDR2	prostaglandin D2 receptor 2
52	ABL1	ABL proto-oncogene 1
53	STS	steroid sulfatase
54	NTRK2	neurotrophic receptor tyrosine kinase 2
55	XIAP	X-linked inhibitor of apoptosis
56	INSR	insulin receptor
57	NFE2L2	NFE2-like bZIP transcription factor 2
58	HDAC4	histone deacetylase 4
59	HDAC9	histone deacetylase 9

Table A2. GO biological processes.

GO	Description	Count	%	Log (*p*-Value)
GO:0009725	response to hormone	28	47.46	−28.2906
GO:0032870	cellular response to hormone stimulus	21	35.59	−22.1297
GO:0048732	gland development	19	32.20	−20.4392
GO:0071396	cellular response to lipid	20	33.90	−20.0435
GO:0043434	response to peptide hormone	18	30.51	−19.8568
GO:1901652	response to peptide	19	32.20	−19.7229
GO:0071417	cellular response to organonitrogen compound	19	32.20	−17.7248
GO:1901699	cellular response to nitrogen compound	19	32.20	−17.2401

Table A2. *Cont.*

GO	Description	Count	%	Log (*p*-Value)
GO:1901653	cellular response to peptide	15	25.42	−16.5512
GO:0071375	cellular response to peptide hormone stimulus	14	23.73	−16.4445
GO:0007167	enzyme-linked receptor protein signaling pathway	18	30.51	−16.0099
GO:0032868	response to insulin	13	22.03	−15.5597
GO:0030335	positive regulation of cell migration	17	28.81	−15.1975
GO:0035270	endocrine system development	11	18.64	−14.8955
GO:2000147	positive regulation of cell motility	17	28.81	−14.872
GO:0030522	intracellular receptor signaling pathway	12	20.34	−14.7579
GO:0040017	positive regulation of locomotion	17	28.81	−14.7092
GO:0007169	transmembrane receptor protein tyrosine kinase signaling pathway	15	25.42	−14.6503
GO:0032869	cellular response to insulin stimulus	11	18.64	−14.1934
GO:0048545	response to steroid hormone	13	22.03	−14.1231
GO:0004672	protein kinase activity	14	23.72	−11.5209
GO:0140297	DNA-binding transcription factor binding	13	22.03	−11.1747
GO:0008134	transcription factor binding	14	23.73	−11.1417
GO:0004879	nuclear receptor activity	7	11.86	−11.0367
GO:0098531	ligand-activated transcription factor activity	7	11.86	−10.9758
GO:0016773	phosphotransferase activity, alcohol group as acceptor	14	23.73	−10.5067
GO:0061629	RNA polymerase II-specific DNA-binding transcription factor binding	11	18.64	−10.2395
GO:0016301	kinase activity	14	23.73	−10.0562
GO:0004955	prostaglandin receptor activity	4	6.78	−8.56851
GO:0019900	kinase binding	13	22.03	−8.5368
GO:0004954	prostanoid receptor activity	4	6.78	−8.37285
GO:0019901	protein kinase binding	12	20.34	−8.04403
GO:0042562	hormone binding	6	10.17	−7.7874
GO:0004953	icosanoid receptor activity	4	6.78	−7.75875
GO:0004674	protein serine/threonine kinase activity	9	15.25	−6.86615
GO:0004713	protein tyrosine kinase activity	6	10.17	−6.52868
GO:0002020	protease binding	6	10.17	−6.49179
GO:0019199	transmembrane receptor protein kinase activity	5	8.47	−6.32271
GO:0019904	protein domain specific binding	10	16.95	−6.32105
GO:0033218	amide binding	8	13.56	−5.94186

Table A3. GO cellular components.

GO	Description	Count	%	Log (*p*-Value)
GO:0045121	membrane raft	9	15.25	−8.37279
GO:0098857	membrane microdomain	9	15.25	−8.35955
GO:0005667	transcription regulator complex	10	16.95	−7.25901
GO:0043235	receptor complex	10	16.95	−7.04516
GO:0044297	cell body	10	16.95	−6.97898
GO:0043025	neuronal cell body	9	15.25	−6.39411
GO:0090575	RNA polymerase II transcription regulator complex	6	10.17	−4.98282
GO:0031252	cell leading edge	7	11.86	−4.73873
GO:0005901	caveola	4	6.78	−4.71441
GO:0030027	lamellipodium	5	8.47	−4.32896
GO:0005911	cell–cell junction	7	11.86	−4.20332
GO:0044853	plasma membrane raft	4	6.78	−4.16185
GO:1902911	protein kinase complex	4	6.78	−3.68335
GO:0030424	axon	7	11.86	−3.58421
GO:0061695	transferase complex, transferring phosphorus-containing groups	5	8.47	−3.47364
GO:0005788	endoplasmic reticulum lumen	5	8.47	−3.44166
GO:0005635	nuclear envelope	6	10.17	−3.39345
GO:0098802	plasma membrane signaling receptor complex	5	8.47	−3.36715
GO:0098552	side of membrane	7	11.86	−3.2816
GO:0098797	plasma membrane protein complex	7	11.86	−3.25701

Table A4. KEGG pathways.

Pathway ID	Pathway Name	Log (*p*-Value)	Count	Gene Hits
hsa05200	Pathways in cancer	−23.1337	22	ABL1, AKT1, XIAP, AR, RHOA, BRAF, CASP3, CDK4, GLI1, GLI2, HIF1A, IGF1R, IL6, KIT, NFE2L2, PIK3CA, PPARG, MAPK1, MAPK3, SHH, STAT3, TGFBR1
hsa05417	Lipid and atherosclerosis	−17.2688	14	AKT1, RHOA, CASP1, CASP3, IL1B, IL6, NFE2L2, PIK3CA, PPARG, MAPK1, MAPK3, STAT3, TNF, NLRP3
hsa04933	AGE-RAGE signaling pathway in diabetic complications	−16.151	11	AKT1, CASP3, CDK4, IL1B, IL6, PIK3CA, MAPK1, MAPK3, STAT3, TGFBR1, TNF
hsa05135	Yersinia infection	−14.6017	11	AKT1, RHOA, CASP1, PTK2B IL1B, IL6, PIK3CA, MAPK1 MAPK3, TNF, NLRP3
hsa05205	Proteoglycans in cancer	−14.248	12	AKT1, RHOA, BRAF, CASP3, HIF1A, IGF1R, PIK3CA, MAPK1, MAPK3, SHH, STAT3, TNF
hsa04625	C-type lectin receptor signaling pathway	−14.0983	10	AKT1, RHOA, CASP1, IL1B, IL6, PIK3CA, MAPK1, MAPK3, TNF, NLRP3
hsa05161	Hepatitis B	−13.7886	11	AKT1, BRAF, CASP3, PTK2B, IL6, PIK3CA, MAPK1, MAPK3, STAT3, TGFBR1, TNF
hsa05163	Human cytomegalovirus infection	−13.7625	12	AKT1, RHOA, CASP3, CDK4, PTK2B, IL1B, IL6, PIK3CA, MAPK1, MAPK3, STAT3, TNF
hsa05133	Pertussis	−13.5622	9	RHOA, CASP1, CASP3, IL1B, IL6, MAPK1, MAPK3, TNF, NLRP3
hsa05164	Influenza A	−13.5279	11	AKT1, CASP1, CASP3, CDK4, IL1B, IL6, PIK3CA, MAPK1, MAPK3, TNF, NLRP3
hsa04068	FoxO signaling pathway	−13.0723	10	AKT1, BRAF, IGF1R, IL6, INSR, PIK3CA, MAPK1, MAPK3, STAT3, TGFBR1
hsa04010	MAPK signaling pathway	−12.2603	12	AKT1, BRAF, CASP3, IGF1R, IL1B, INSR, KIT NTRK2, MAPK1, MAPK3, TGFBR1, TNF
hsa05160	Hepatitis C	−12.249	10	AKT1, BRAF, CASP3, CDK4, PIK3CA, PPARA, MAPK1, MAPK3, STAT3, TNF
hsa04931	Insulin resistance	−12.1443	9	AKT1, IL6, INSR, PIK3CA, PPARA, PTPN1, STAT3, TNF, NR1H2
hsa04066	HIF-1 signaling pathway	−12.1075	9	AKT1, HIF1A, IGF1R, IL6, INSR, PIK3CA, MAPK1 MAPK3, STAT3
hsa04668	TNF signaling pathway	−11.9288	9	AKT1, XIAP, CASP3, IL1B, IL6, PIK3CA, MAPK1, MAPK3, TNF
hsa05132	Salmonella infection	−11.7368	11	AKT1, RHOA, CASP1 CASP3, IL1B, IL6, PIK3CA, MAPK1, MAPK3, TNF, NLRP3
hsa05212	Pancreatic cancer	−11.6678	8	AKT1, BRAF, CDK4, PIK3CA, MAPK1, MAPK3, STAT3, TGFBR1
hsa05220	Chronic myeloid leukemia	−11.6678	8	ABL1, AKT1, BRAF, CDK4, PIK3CA, MAPK1, MAPK3, TGFBR1
hsa01521	EGFR tyrosine kinase inhibitor resistance	−11.5287	8	AKT1, BRAF, IGF1R, IL6, PIK3CA, MAPK1, MAPK3, STAT3

References

1. Schwartzenfeld, D.M.; Karamikian, J. Hair Transplantation. In *Plastic Surgery Secrets Plus*; Elsevier: Amsterdam, The Netherlands, 2010; pp. 123–127.
2. Frith, H.; Jankowski, G.S. Psychosocial Impact of Androgenetic Alopecia on Men: A Systematic Review and Meta-Analysis. *Psychol. Health Med.* **2023**, *29*, 822–842. [CrossRef] [PubMed]
3. Shin, Y.S.; Karna, K.K.; Choi, B.R.; Park, J.K. Finasteride and Erectile Dysfunction in Patients with Benign Prostatic Hyperplasia or Male Androgenetic Alopecia. *World J. Men's Health* **2019**, *37*, 157. [CrossRef]
4. BinJadeed, H.; Almudimeegh, A.M.; Alomran, S.A.; Alshathry, A.H. A Case of Contact Allergic Dermatitis to Topical Minoxidil. *Cureus* **2021**, *13*, e12510. [CrossRef]
5. Herman, A.; Herman, A.P. Mechanism of Action of Herbs and Their Active Constituents Used in Hair Loss Treatment. *Fitoterapia* **2016**, *114*, 18–25. [CrossRef]
6. Nurcholis, W.; Priosoeryanto, B.P.; Purwakusumah, E.D.; Katayama, T.; Suzuki, T. Antioxidant, Cytotoxic Activities and Total Phenolic Content of Four Indonesian Medicinal Plants. *J. Kim. Val.* **2012**, *2*, 4. [CrossRef]

7. Zohmachhuana, A.; Malsawmdawngliana; Lalnunmawia, F.; Mathipi, V.; Lalrinzuali, K.; Kumar, N.S. *Curcuma aeruginosa* Roxb. Exhibits Cytotoxicity in A-549 and HeLa Cells by Inducing Apoptosis through Caspase-Dependent Pathways. *Biomed. Pharmacother.* **2022**, *150*, 113039. [CrossRef]
8. Akarchariya, N.; Sirilun, S.; Julsrigival, J.; Chansakaowa, S. Chemical Profiling and Antimicrobial Activity of Essential Oil from *Curcuma aeruginosa* Roxb., Curcuma Glans K. Larsen & J. Mood and Curcuma Cf. Xanthorrhiza Roxb. Collected in Thailand. *Asian Pac. J. Trop. Biomed.* **2017**, *7*, 881–885. [CrossRef]
9. Sillapachaiyaporn, C.; Rangsinth, P.; Nilkhet, S.; Moungkote, N.; Chuchawankul, S. HIV-1 Protease and Reverse Transcriptase Inhibitory Activities of *Curcuma aeruginosa* Roxb. Rhizome Extracts and the Phytochemical Profile Analysis: In Vitro and In Silico Screening. *Pharmaceuticals* **2021**, *14*, 1115. [CrossRef]
10. Thaina, P.; Tungcharoen, P.; Wongnawa, M.; Reanmongkol, W.; Subhadhirasakul, S. Uterine Relaxant Effects of *Curcuma aeruginosa* Roxb. Rhizome Extracts. *J. Ethnopharmacol.* **2009**, *121*, 433–443. [CrossRef]
11. Suphrom, N.; Pumthong, G.; Khorana, N.; Waranuch, N.; Limpeanchob, N.; Ingkaninan, K. Anti-Androgenic Effect of Sesquiterpenes Isolated from the Rhizomes of *Curcuma aeruginosa* Roxb. *Fitoterapia* **2012**, *83*, 864–871. [CrossRef]
12. Pumthong, G.; Asawanonda, P.; Varothai, S.; Jariyasethavong, V.; Triwongwaranat, D.; Suthipinittharm, P.; Ingkaninan, K.; Leelapornpisit, P.; Waranuch, N. *Curcuma aeruginosa*, a Novel Botanically Derived 5α-Reductase Inhibitor in the Treatment of Male-Pattern Baldness: A Multicenter, Randomized, Double-Blind, Placebo-Controlled Study. *J. Dermatol. Treat.* **2012**, *23*, 385–392. [CrossRef] [PubMed]
13. Srivilai, J.; Waranuch, N.; Tangsumranjit, A.; Khorana, N.; Ingkaninan, K. Germacrone and Sesquiterpene-Enriched Extracts from *Curcuma aeruginosa* Roxb. Increase Skin Penetration of Minoxidil, a Hair Growth Promoter. *Drug Deliv. Transl. Res.* **2018**, *8*, 140–149. [CrossRef]
14. Li, S.; Zhang, B. Traditional Chinese Medicine Network Pharmacology: Theory, Methodology and Application. *Chin. J. Nat. Med.* **2013**, *11*, 110–120. [CrossRef] [PubMed]
15. Liu, C.; Liu, L.; Li, J.; Zhang, Y.; Meng, D.-L. Virtual Screening of Active Compounds from Jasminum Lanceolarium and Potential Targets against Primary Dysmenorrhea Based on Network Pharmacology. *Nat. Prod. Res.* **2021**, *35*, 5853–5856. [CrossRef] [PubMed]
16. Vivek-Ananth, R.P.; Mohanraj, K.; Sahoo, A.K.; Samal, A. IMPPAT 2.0: An Enhanced and Expanded Phytochemical Atlas of Indian Medicinal Plants. *ACS Omega* **2023**, *8*, 8827–8845. [CrossRef] [PubMed]
17. Daina, A.; Michielin, O.; Zoete, V. SwissADME: A Free Web Tool to Evaluate Pharmacokinetics, Drug-Likeness and Medicinal Chemistry Friendliness of Small Molecules. *Sci. Rep.* **2017**, *7*, 42717. [CrossRef]
18. Daina, A.; Michielin, O.; Zoete, V. SwissTargetPrediction: Updated Data and New Features for Efficient Prediction of Protein Targets of Small Molecules. *Nucleic Acids Res.* **2019**, *47*, W357–W364. [CrossRef]
19. Wang, J.-H.; Zhao, L.-F.; Wang, H.-F.; Wen, Y.-T.; Jiang, K.-K.; Mao, X.-M.; Zhou, Z.-Y.; Yao, K.-T.; Geng, Q.-S.; Guo, D.; et al. GenCLiP 3: Mining Human Genes' Functions and Regulatory Networks from PubMed Based on Co-Occurrences and Natural Language Processing. *Bioinformatics* **2020**, *36*, 1973–1975. [CrossRef]
20. Piñero, J.; Bravo, À.; Queralt-Rosinach, N.; Gutiérrez-Sacristán, A.; Deu-Pons, J.; Centeno, E.; García-García, J.; Sanz, F.; Furlong, L.I. DisGeNET: A Comprehensive Platform Integrating Information on Human Disease-Associated Genes and Variants. *Nucleic Acids Res.* **2017**, *45*, D833–D839. [CrossRef]
21. Amberger, J.S.; Bocchini, C.A.; Schiettecatte, F.; Scott, A.F.; Hamosh, A. OMIM.Org: Online Mendelian Inheritance in Man (OMIM®), an Online Catalog of Human Genes and Genetic Disorders. *Nucleic Acids Res.* **2015**, *43*, D789–D798. [CrossRef]
22. Safran, M.; Dalah, I.; Alexander, J.; Rosen, N.; Iny Stein, T.; Shmoish, M.; Nativ, N.; Bahir, I.; Doniger, T.; Krug, H.; et al. GeneCards Version 3: The Human Gene Integrator. *Database* **2010**, *2010*, baq020. [CrossRef] [PubMed]
23. Szklarczyk, D.; Franceschini, A.; Kuhn, M.; Simonovic, M.; Roth, A.; Minguez, P.; Doerks, T.; Stark, M.; Muller, J.; Bork, P.; et al. The STRING Database in 2011: Functional Interaction Networks of Proteins, Globally Integrated and Scored. *Nucleic Acids Res.* **2011**, *39*, D561–D568. [CrossRef]
24. Zhou, Y.; Zhou, B.; Pache, L.; Chang, M.; Khodabakhshi, A.H.; Tanaseichuk, O.; Benner, C.; Chanda, S.K. Metascape Provides a Biologist-Oriented Resource for the Analysis of Systems-Level Datasets. *Nat. Commun.* **2019**, *10*, 1523. [CrossRef] [PubMed]
25. Liu, Y.; Yang, X.; Gan, J.; Chen, S.; Xiao, Z.-X.; Cao, Y. CB-Dock2: Improved Protein-Ligand Blind Docking by Integrating Cavity Detection, Docking and Homologous Template Fitting. *Nucleic Acids Res.* **2022**, *50*, W159–W164. [CrossRef]
26. Sari, A.P.; Supratman, U. Phytochemistry and Biological Activities of *Curcuma aeruginosa* (Roxb.). *Indones. J. Chem.* **2022**, *22*, 576–598. [CrossRef]
27. Martin, Y.C. A Bioavailability Score. *J. Med. Chem.* **2005**, *48*, 3164–3170. [CrossRef] [PubMed]
28. Saad, S.; Cavelier-Balloy, B.; Smadja, J.; Assouly, P.; Reygagne, P. Inflammatory Complications after Hair Transplantation: Report of 10 Cases. *J. Cosmet. Dermatol.* **2022**, *21*, 5938–5941. [CrossRef]
29. Almohanna, H.M.; Perper, M.; Tosti, A. Safety Concerns When Using Novel Medications to Treat Alopecia. *Expert Opin. Drug Saf.* **2018**, *17*, 1115–1128. [CrossRef]
30. Dou, J.; Zhang, Z.; Xu, X.; Zhang, X. Exploring the Effects of Chinese Herbal Ingredients on the Signaling Pathway of Alopecia and the Screening of Effective Chinese Herbal Compounds. *J. Ethnopharmacol.* **2022**, *294*, 115320. [CrossRef]
31. Fan, X.; Chen, J.; Zhang, Y.; Wang, S.; Zhong, W.; Yuan, H.; Wu, X.; Wang, C.; Zheng, Y.; Wei, Y.; et al. Alpinetin Promotes Hair Regeneration via Activating Hair Follicle Stem Cells. *Chin. Med.* **2022**, *17*, 63. [CrossRef]

32. Martinez-Jacobo, L.; Ancer-Arellano, C.I.; Ortiz-Lopez, R.; Salinas-Santander, M.; Villarreal-Villarreal, C.D.; Ancer-Rodriguez, J.; Camacho-Zamora, B.; Zomosa-Signoret, V.; Medina-De la Garza, C.E.; Ocampo-Candiani, J.; et al. Evaluation of the Expression of Genes Associated with Inflammation and Apoptosis in Androgenetic Alopecia by Targeted RNA-Seq. *Skin Appendage Disord.* **2018**, *4*, 268–273. [CrossRef] [PubMed]
33. Wang, G.; Wang, Z.; Zhang, J.; Shen, Y.; Hou, X.; Su, L.; Chen, W.; Chen, J.; Guo, X.; Song, H. Treatment of Androgenetic Alopecia by Exosomes Secreted from Hair Papilla Cells and the Intervention Effect of LTF. *J. Cosmet. Dermatol.* **2023**, *22*, 2996–3007. [CrossRef] [PubMed]
34. Chen, Y.; Fan, Z.; Wang, X.; Mo, M.; Zeng, S.B.; Xu, R.-H.; Wang, X.; Wu, Y. PI3K/Akt Signaling Pathway Is Essential for de Novo Hair Follicle Regeneration. *Stem Cell Res. Ther.* **2020**, *11*, 144. [CrossRef] [PubMed]
35. Sun, M.; Yang, L.; Feldman, R.I.; Sun, X.; Bhalla, K.N.; Jove, R.; Nicosia, S.V.; Cheng, J.Q. Activation of Phosphatidylinositol 3-Kinase/Akt Pathway by Androgen through Interaction of P85α, Androgen Receptor, and Src. *J. Biol. Chem.* **2003**, *278*, 42992–43000. [CrossRef]
36. Hibberts, N.; Howell, A.; Randall, V. Balding Hair Follicle Dermal Papilla Cells Contain Higher Levels of Androgen Receptors than Those from Non-Balding Scalp. *J. Endocrinol.* **1998**, *156*, 59–65. [CrossRef] [PubMed]
37. Ellis, J.A.; Stebbing, M.; Harrap, S.B. Polymorphism of the Androgen Receptor Gene Is Associated with Male Pattern Baldness. *J. Investig. Dermatol.* **2001**, *116*, 452–455. [CrossRef] [PubMed]
38. Sawaya, M.E.; Price, V.H. Different Levels of 5α-Reductase Type I and II, Aromatase, and Androgen Receptor in Hair Follicles of Women and Men with Androgenetic Alopecia. *J. Investig. Dermatol.* **1997**, *109*, 296–300. [CrossRef] [PubMed]
39. Hodgins, M.B.; Choudhry, R.; Parker, G.; Oliver, R.F.; Jahoda, C.A.B.; Withers, A.P.; Brinkmann, A.O.; Van Der Kwast, T.H.; Boersma, W.J.A.; Lammers, K.M.; et al. Androgen Receptors in Dermal Papilla Cells of Scalp Hair Follicles in Male Pattern Baldness. *Ann. N. Y. Acad. Sci.* **1991**, *642*, 448–451. [CrossRef]
40. Mahmoud, E.A.; Elgarhy, L.H.; Hasby, E.A.; Mohammad, L. Dickkopf-1 Expression in Androgenetic Alopecia and Alopecia Areata in Male Patients. *Am. J. Dermatopathol.* **2019**, *41*, 122–127. [CrossRef]
41. Tsuji, Y.; Denda, S.; Soma, T.; Raftery, L.; Momoi, T.; Hibino, T. A Potential Suppressor of TGF-β Delays Catagen Progression in Hair Follicles. *J. Investig. Dermatol. Symp. Proc.* **2003**, *8*, 65–68. [CrossRef]
42. Kwack, M.H.; Ahn, J.S.; Kim, M.K.; Kim, J.C.; Sung, Y.K. Dihydrotestosterone-Inducible IL-6 Inhibits Elongation of Human Hair Shafts by Suppressing Matrix Cell Proliferation and Promotes Regression of Hair Follicles in Mice. *J. Investig. Dermatol.* **2012**, *132*, 43–49. [CrossRef]
43. Ramot, Y.; Alam, M.; Oláh, A.; Bíró, T.; Ponce, L.; Chéret, J.; Bertolini, M.; Paus, R. Peroxisome Proliferator–Activated Receptor-Γ−Mediated Signaling Regulates Mitochondrial Energy Metabolism in Human Hair Follicle Epithelium. *J. Investig. Dermatol.* **2018**, *138*, 1656–1659. [CrossRef]
44. Kwack, M.H.; Sung, Y.K.; Chung, E.J.; Im, S.U.; Ahn, J.S.; Kim, M.K.; Kim, J.C. Dihydrotestosterone-Inducible Dickkopf 1 from Balding Dermal Papilla Cells Causes Apoptosis in Follicular Keratinocytes. *J. Investig. Dermatol.* **2008**, *128*, 262–269. [CrossRef]
45. Winiarska, A.; Mandt, N.; Kamp, H.; Hossini, A.; Seltmann, H.; Zouboulis, C.C.; Blume-Peytavi, U. Effect of 5α-Dihydrotestosterone and Testosterone on Apoptosis in Human Dermal Papilla Cells. *Skin Pharmacol. Physiol.* **2006**, *19*, 311–321. [CrossRef]
46. Sano, S.; Kira, M.; Takagi, S.; Yoshikawa, K.; Takeda, J.; Itami, S. Two Distinct Signaling Pathways in Hair Cycle Induction: Stat3-Dependent and -Independent Pathways. *Proc. Natl. Acad. Sci. USA* **2000**, *97*, 13824–13829. [CrossRef]
47. Kim, D.J.; Kataoka, K.; Rao, D.; Kiguchi, K.; Cotsarelis, G.; DiGiovanni, J. Targeted Disruption of Stat3 Reveals a Major Role for Follicular Stem Cells in Skin Tumor Initiation. *Cancer Res.* **2009**, *69*, 7587–7594. [CrossRef]
48. Rao, D.; Macias, E.; Carbajal, S.; Kiguchi, K.; DiGiovanni, J. Constitutive Stat3 Activation Alters Behavior of Hair Follicle Stem and Progenitor Cell Populations. *Mol. Carcinog.* **2015**, *54*, 121–133. [CrossRef]
49. Seo, J.; Yan, L.; Kageyama, T.; Nanmo, A.; Chun, Y.-S.; Fukuda, J. Hypoxia Inducible Factor-1α Promotes Trichogenic Gene Expression in Human Dermal Papilla Cells. *Sci. Rep.* **2023**, *13*, 1478. [CrossRef]
50. Bukowiecki, J.; Pförringer, D.; Thor, D.; Duscher, D.; Brett, E. HIF-1α Stimulators Function Equally to Leading Hair Loss Agents in Enhancing Dermal Papilla Growth. *Skin Pharmacol. Physiol.* **2020**, *33*, 309–316. [CrossRef] [PubMed]
51. Akilli Öztürk, Ö.; Pakula, H.; Chmielowiec, J.; Qi, J.; Stein, S.; Lan, L.; Sasaki, Y.; Rajewsky, K.; Birchmeier, W. Gab1 and Mapk Signaling Are Essential in the Hair Cycle and Hair Follicle Stem Cell Quiescence. *Cell Rep.* **2015**, *13*, 561–572. [CrossRef] [PubMed]
52. Choi, M.; Choi, S.-J.; Jang, S.; Choi, H.-I.; Kang, B.-M.; Hwang, S.T.; Kwon, O. Shikimic Acid, a Mannose Bioisostere, Promotes Hair Growth with the Induction of Anagen Hair Cycle. *Sci. Rep.* **2019**, *9*, 17008. [CrossRef] [PubMed]
53. Stamatas, G.N.; Wu, J.; Pappas, A.; Mirmirani, P.; McCormick, T.S.; Cooper, K.D.; Consolo, M.; Schastnaya, J.; Ozerov, I.V.; Aliper, A.; et al. An Analysis of Gene Expression Data Involving Examination of Signaling Pathways Activation Reveals New Insights into the Mechanism of Action of Minoxidil Topical Foam in Men with Androgenetic Alopecia. *Cell Cycle* **2017**, *16*, 1578–1584. [CrossRef]
54. Deng, Z.; Chen, M.; Liu, F.; Wang, Y.; Xu, S.; Sha, K.; Peng, Q.; Wu, Z.; Xiao, W.; Liu, T.; et al. Androgen Receptor–Mediated Paracrine Signaling Induces Regression of Blood Vessels in the Dermal Papilla in Androgenetic Alopecia. *J. Investig. Dermatol.* **2022**, *142*, 2088–2099.e9. [CrossRef]

55. Garza, L.A.; Liu, Y.; Yang, Z.; Alagesan, B.; Lawson, J.A.; Norberg, S.M.; Loy, D.E.; Zhao, T.; Blatt, H.B.; Stanton, D.C.; et al. Prostaglandin D_2 Inhibits Hair Growth and Is Elevated in Bald Scalp of Men with Androgenetic Alopecia. *Sci. Transl. Med.* **2012**, *4*, 126ra34. [CrossRef] [PubMed]
56. Jung, Y.H.; Chae, C.W.; Choi, G.E.; Shin, H.C.; Lim, J.R.; Chang, H.S.; Park, J.; Cho, J.H.; Park, M.R.; Lee, H.J.; et al. Cyanidin 3-O-Arabinoside Suppresses DHT-Induced Dermal Papilla Cell Senescence by Modulating P38-Dependent ER-Mitochondria Contacts. *J. Biomed. Sci.* **2022**, *29*, 17. [CrossRef] [PubMed]
57. Oh, H.S.; Smart, R.C. An Estrogen Receptor Pathway Regulates the Telogen-Anagen Hair Follicle Transition and Influences Epidermal Cell Proliferation. *Proc. Natl. Acad. Sci. USA* **1996**, *93*, 12525–12530. [CrossRef] [PubMed]
58. Liedert, A.; Nemitz, C.; Haffner-Luntzer, M.; Schick, F.; Jakob, F.; Ignatius, A. Effects of Estrogen Receptor and Wnt Signaling Activation on Mechanically Induced Bone Formation in a Mouse Model of Postmenopausal Bone Loss. *Int. J. Mol. Sci.* **2020**, *21*, 8301. [CrossRef] [PubMed]
59. Choi, B.Y. Targeting Wnt/β-Catenin Pathway for Developing Therapies for Hair Loss. *Int. J. Mol. Sci.* **2020**, *21*, 4915. [CrossRef] [PubMed]
60. Bellanti, F.; Matteo, M.; Rollo, T.; De Rosario, F.; Greco, P.; Vendemiale, G.; Serviddio, G. Sex Hormones Modulate Circulating Antioxidant Enzymes: Impact of Estrogen Therapy. *Redox Biol.* **2013**, *1*, 340–346. [CrossRef]
61. Choi, S.; Zhang, B.; Ma, S.; Gonzalez-Celeiro, M.; Stein, D.; Jin, X.; Kim, S.T.; Kang, Y.-L.; Besnard, A.; Rezza, A.; et al. Corticosterone Inhibits GAS6 to Govern Hair Follicle Stem-Cell Quiescence. *Nature* **2021**, *592*, 428–432. [CrossRef]
62. Raman, M.; Chen, W.; Cobb, M.H. Differential Regulation and Properties of MAPKs. *Oncogene* **2007**, *26*, 3100–3112. [CrossRef] [PubMed]
63. Kim, J.; Kim, S.R.; Choi, Y.-H.; Shin, J.Y.; Kim, C.D.; Kang, N.-G.; Park, B.C.; Lee, S. Quercitrin Stimulates Hair Growth with Enhanced Expression of Growth Factors via Activation of MAPK/CREB Signaling Pathway. *Molecules* **2020**, *25*, 4004. [CrossRef]
64. Wang, X.; Liu, Y.; He, J.; Wang, J.; Chen, X.; Yang, R. Regulation of signaling pathways in hair follicle stem cells. *Burns Trauma* **2022**, *10*, tkac022. [CrossRef]
65. Huang, H.-C.; Lin, H.; Huang, M.-C. Lactoferrin Promotes Hair Growth in Mice and Increases Dermal Papilla Cell Proliferation through Erk/Akt and Wnt Signaling Pathways. *Arch. Dermatol. Res.* **2019**, *311*, 411–420. [CrossRef] [PubMed]
66. Choi, Y.K.; Kang, J.-I.; Hyun, J.W.; Koh, Y.S.; Kang, J.-H.; Hyun, C.-G.; Yoon, K.-S.; Lee, K.S.; Lee, C.M.; Kim, T.Y.; et al. Myristoleic Acid Promotes Anagen Signaling by Autophagy through Activating Wnt/β-Catenin and ERK Pathways in Dermal Papilla Cells. *Biomol. Ther.* **2021**, *29*, 211–219. [CrossRef]
67. Bikkavilli, R.K.; Feigin, M.E.; Malbon, C.C. P38 Mitogen-Activated Protein Kinase Regulates Canonical Wnt–β-Catenin Signaling by Inactivation of GSK3β. *J. Cell Sci.* **2008**, *121*, 3598–3607. [CrossRef]
68. He, Y.; Cai, C.; Sun, S.; Wang, X.; Li, W.; Li, H. Effect of JNK Inhibitor SP600125 on Hair Cell Regeneration in Zebrafish (*Danio rerio*) Larvae. *Oncotarget* **2016**, *7*, 51640–51650. [CrossRef] [PubMed]
69. Yum, S.; Jeong, S.; Kim, D.; Lee, S.; Kim, W.; Yoo, J.-W.; Kim, J.-A.; Kwon, O.; Kim, D.-D.; Min, D.; et al. Minoxidil Induction of VEGF Is Mediated by Inhibition of HIF-Prolyl Hydroxylase. *Int. J. Mol. Sci.* **2017**, *19*, 53. [CrossRef]
70. Imamura, Y.; Tomita, S.; Imanishi, M.; Kihira, Y.; Ikeda, Y.; Ishizawa, K.; Tsuchiya, K.; Tamaki, T. HIF-2α/ARNT Complex Regulates Hair Development via Induction of $P21^{Waf1/Cip1}$ and $P27^{Kip1}$. *FASEB J.* **2014**, *28*, 2517–2524. [CrossRef]
71. Pagani, A.; Aitzetmüller, M.M.; Brett, E.A.; König, V.; Wenny, R.; Thor, D.; Radtke, C.; Huemer, G.M.; Machens, H.-G.; Duscher, D. Skin Rejuvenation through HIF-1α Modulation. *Plast. Reconstr. Surg.* **2018**, *141*, 600e–607e. [CrossRef]
72. Thor, D.; Pagani, A.; Bukowiecki, J.; Houschyar, K.S.; Kølle, S.-F.T.; Wyles, S.P.; Duscher, D. A Novel Hair Restoration Technology Counteracts Androgenic Hair Loss and Promotes Hair Growth in A Blinded Clinical Trial. *J. Clin. Med.* **2023**, *12*, 470. [CrossRef] [PubMed]
73. Ceruti, J.M.; Leirós, G.J.; Balañá, M.E. Androgens and Androgen Receptor Action in Skin and Hair Follicles. *Mol. Cell. Endocrinol.* **2018**, *465*, 122–133. [CrossRef] [PubMed]
74. O'Shaughnessy, P.J.; Antignac, J.P.; Le Bizec, B.; Morvan, M.-L.; Svechnikov, K.; Söder, O.; Savchuk, I.; Monteiro, A.; Soffientini, U.; Johnston, Z.C.; et al. Alternative (Backdoor) Androgen Production and Masculinization in the Human Fetus. *PLoS Biol.* **2019**, *17*, e3000002. [CrossRef] [PubMed]
75. Fukami, M.; Homma, K.; Hasegawa, T.; Ogata, T. Backdoor Pathway for Dihydrotestosterone Biosynthesis: Implications for Normal and Abnormal Human Sex Development. *Dev. Dyn.* **2013**, *242*, 320–329. [CrossRef]
76. Shen, Y.; Zhu, Y.; Zhang, L.; Sun, J.; Xie, B.; Zhang, H.; Song, X. New Target for Minoxidil in the Treatment of Androgenetic Alopecia. *Drug Des. Dev. Ther.* **2023**, *17*, 2537–2547. [CrossRef]

Disclaimer/Publisher's Note: The statements, opinions and data contained in all publications are solely those of the individual author(s) and contributor(s) and not of MDPI and/or the editor(s). MDPI and/or the editor(s) disclaim responsibility for any injury to people or property resulting from any ideas, methods, instructions or products referred to in the content.